Qeios

Modelling Skeletal Muscle Motor Unit Recruitment Contributions To Contractile Function: Part 1 - Velocity, Force and Power

Lucy R. Mulligan[1], Gerhard Nygaard[2], Justin Holland[1], Robert A. Robergs[1]

Address for correspondence: Robert Robergs, School of Exercise and Nutrition Sciences, O Block, A Wing, Level 4, Room A420, Faculty of Health, Queensland University of Technology, Kelvin Grove, Queensland, 4059, Australia; Phone: +61 7 3138 0339; Email: rob.robergs@qut.edu.au

[1] School of Exercise and Nutrition Sciences, O Block, A Wing, Level 4, Room A420, Faculty of Health, Queensland University of Technology, Kelvin Grove, Queensland, 4059, Australia

[2] Department of Computer Science, Electrical Engineering and Mathematical Sciences, Western Norway University of Applied Sciences, Høgskulen på Vestlandet, Postbox 7030, 5020 Bergen, Norway.

ORCID #s

Robert A. Robergs : 0000-0002-7741-8136

Gerhard Nygaard : 0000-0003-2349-4659

Justin Holland : 0000-0001-6393-4319

https://doi.org/10.32388/VREACR

Abstract

There is no current method that can directly measure in-vivo human motor unit recruitment and their individual incremental contributions to muscle contractile velocity, force and power. The purpose of this research was to 1) acquire previously published data of single fibre contractile velocity, force and power for the different skeletal muscle fibre types, corrected for muscle temperature, 2) develop a computational model of motor unit recruitment spanning the 5 fibre type categories (types I, I-IIa, IIa, IIab, and IIb) and four different slow to fast twitch proportions (80-20, 60-40, 40-60, 20-80% ST-FT, respectively), and 3) use the model to compute changes in motor unit contributions to contractile velocity, force and power. The order of motor unit recruitment was based upon motor unit size and ranged from 85 (type-I) to 207 (type IIb) fibres·unit^{-1}. The total number of motor units across the four categories were 3,582, 3,308, 3,041, and 2,757, respectively. Data for 20 vs 100% recruitment for contractile velocity of the 80-20% ST-FT were 0.055 vs 0.09 m·s^{-1}, respectively, and for 20-80% ST-FT were 0.0589 vs 0.1569 m·s^{-1}, respectively. Contractile force data were 28.065 vs 202.01 N, and 28.065 vs 248.14 N, respectively. Contractile power data were 1.545 vs 18.136 Watts, and 1.421 vs 38.957 Watts, respectively. The model succeeded in transferring data from single muscle fibre to motor unit and whole muscle contraction kinematics. Such modelling has future applications to the energetics of muscle contraction at the motor unit and muscle fibre level, and for guiding robotic replication of human muscle contractile function.

Keywords: Fibre type; Motor unit; Myosin heavy chain; Skeletal muscle; Contraction; LabVIEW

Running head: Motor Unit Recruitment Determinants To Muscle Contractile Function

Introduction

Skeletal muscle is a highly organized tissue, where the entire muscle is divided into structural and functional divisions. For example, the largest muscle of the thigh, the vastus lateralis, can have up to 405,000 muscle fibres (1). These muscle fibres are functionally organized into motor units, where each motor unit could comprise between tens to hundreds of muscle fibres, each connected to the central nervous system by the divergence of their motor nerve. Consequently, a motor unit is characterised by morphological and functional features of the motor nerve, neuromuscular junctions, and the contractile and metabolic properties of the skeletal muscle fibres it innervates.

During muscle contraction, each of the motor units that are recruited contract maximally according to the "All Or Nothing" principle so that the number and type of motor units recruited dictates the overall muscle metabolic and contractile profile. Furthermore, as best as can be inferred from early animal research, human motor units are recruited in a sequenced order based on the size of the motor nerve cell body, nerve axon, number of muscle fibres per unit, and contractile and metabolic capacities of the muscle fibres (Size Principle), where the smallest motor units (slow twitch) are recruited first, followed by the added recruitment of progressively larger fast twitch motor units (2).

Despite this well-known morphological and functional detail, for years, human skeletal muscle has been represented in models for biochemical studies and muscle kinematics and kinetics as a homogenous "Black Box" (3-6). In other words, there was no recognition of the differences in contribution of different motor units to the mechanical or biochemical processes involved during muscle contractions. An illustrative representation of such a "Black Box" model has been developed and is presented in Figure 1.

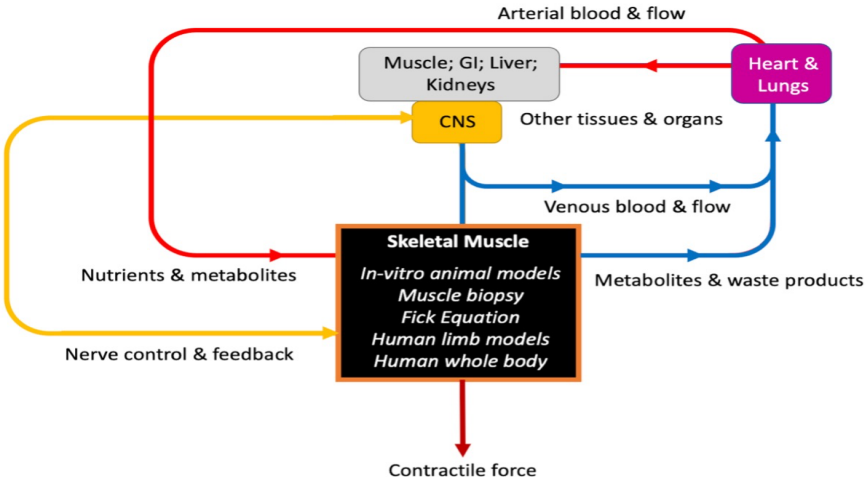

Figure 1: A devised "Black Box" model that has been consistently used to represent skeletal muscle in multiple research methods and data interpretations such as in-vitro animal models, human and animal muscle biopsy, the Fick Equation, human limb and whole-body investigations of physiology and metabolic biochemistry, and past models of progressively increasing skeletal muscle contractile force.

The "Black Box" model only allows a research-driven understanding of muscle function that conforms to entire muscle contraction independent of isolated contributions of progressively changing motor unit recruitment of motor units that differ in contractile function (force, velocity, and power) and the metabolic energy systems that support these functions. This reinforces a view of skeletal muscle function to be that of the muscle as a single unit, whereas as previously explained, skeletal muscle functions by the ordered involvement (recruitment) of thousands of motor units that can have remarkably different contractile and metabolic capacities. The sustained use of the "Black Box" model prevents original investigation and new discovery of the more complex features inherent in skeletal muscle contraction that could have very different determinants to overall muscle power production and cellular driven metabolism.

There are numerous methods to differentiate the muscle fibres of different motor unit categories. Following the discovery of contraction speed correlating with the adenosine triphosphatase (ATPase) activity of the muscle's myosin, histochemical staining by Brooke and Kaiser (7) allowed grouping of these fibres as type I ("slow-twitch") and types IIa ("fast twitch oxidative"), and IIb ("fast-twitch glycolytic"). Further developments to muscle fibre type categorization have been made based on the

myosin heavy chain (MHC) isoform composition. This was done through electrophoretic separation of the MHCs, identifying hybrids and broadening the spectrum of fibre types that exist (8). In a study by Bottinelli et al. (9) of the force-velocity properties of different categories of muscle fibres, myosin heavy chain isoforms chosen to best represent the fibres of this "spectrum" included the myosin expressions of type I, I-IIa, IIa, IIab, and IIb. Of these categorise, type I and I-IIa were considered "slow-twitch", and type IIa, IIab, and IIb were considered "fast-twitch". Table 1 identifies the differences in mechanical parameters of each fibre type.

Table 1: Myosin heavy chain fibre types and their comparative features from derived data (4).

	Type I	**Type I-IIa**	**Type IIa**	**Type IIab**	**Type IIb**
Maximum shortening velocity ($sL \cdot s^{-1}$)	0.264 ± 0.089	0.521 ± 0.149	1.121 ± 0.361	2.139 ± 0.453	2.418 ± 1.497
Force-velocity relationship (no units)	0.032 ± 0.024	0.030 ± 0.017	0.063 ± 0.029	0.060 ± 0.016	0.072 ± 0.035
Specific tension ($kN \cdot m^2$)	43.77 ± 21.90	50.97 ± 14.78	60.64 ± 34.86	64.73 ± 14.48	61.84 ± 14.49
Cross-sectional Area (μm^2)	9278 ± 3496	8569 ± 3211	7922 ± 2845	5492 ± 1167	6294 ± 2159

($sL \cdot s^{-1}$ = fibre segment length per second); data collected at a temperature of 12 °C.

While there have been numerous efforts to model human skeletal muscle contractile function and its related metabolic and kinematic functions, with all scrutinized by Hawkins and Hull (10), all were completed pre-1990 and as such not fully informed by differences in the contractile performance of the varied muscle fibre types or the fibre and motor unit numbers of a human muscle (1,11-15). From a historical perspective, the same concerns have and continue to be pertinent to the model of muscle contractile force production first published in 1938 by Hill (6). Such a model has been refined to current time yet is constrained by how it is based on whole muscle function and as such has poor generalizability to in-vivo muscle contraction, which as previously explained, is based on the sequential and ordered recruitment of motor units. Nevertheless, there are some more recent notable efforts of modelling muscle contraction that are worth mentioning.

Hawkins and Hull (10) used electromyographic and muscle force data of the triceps brachii to estimate muscle fibre recruitment of established proportions of three fibre types (type I, IIa and IIb) and assumed fibre pennation angles. The model was relatively accurate in estimating the actual force, though this was to be expected considering that the muscle activation variable of their equation was largely based on the actual measured forces of the experimental data used. In other words, they used measured force and EMG data as variables in their modelling to estimate contractile force from EMG measured measurements during added contractile efforts at 10% increments (10 - 100%).

Cheng et al. (4) developed a computational method (Virtual Muscle™ built in MATLAB) to ascertain the influence of muscle properties on the control of motor function. A component of this model was the presence of four compartments of muscle based on their fibre type, and where each were differentiated by the firing frequency associated with 50% recruitment. The firing frequency was presented as a linear function across the four compartments, which represented different slow to fast twitch muscle fibre categories. Song et al. (16) expanded on the operation of the Virtual Muscle, yet computation of resulting forces and power were not motor unit specific. Rather, multiple motor units of a similar type were combined into a total motor unit pool, and this composite was linearly controlled in recruitment.

Finally, Potvin and Fuglevand (17) investigated muscle contractile fatigue through the development of a phenomenological model of motor unit fatigue during isometric contractions. The model used a prior model of muscle motor unit pools (18) to estimate contraction times to failure during isometric contractions across different contraction forces (% MVC). Thus, the focus of the research was not on the quantification or pattern of changes for the contribution of the different motor units to contractile force, but in the time dependent profile of the force production for muscle of different % motor unit type proportions.

While some of the prior models did focus on comparing results for theoretical muscles of different motor unit proportions, none provided clear computational methods and related results for applying known muscle fibre contractile force and power of the different fibre types, in addition to the influence of different motor unit recruitment capacities to gross muscle force and power. It was

hypothesized that if a new model was developed to adhere to the realities of the All or None and Size principles of muscle contraction and motor unit recruitment, along with understanding the different mechanical properties of the muscle fibres of the different motor units, there could be new knowledge gained for how the different fibre types contribute to muscle contractile force and power. This has further relevance to future additions to the model for physiological and biochemical functions and measurements such as ATP turnover, oxygen consumption (VO_2), carbon dioxide production (VCO_2) and metabolite production and accumulation such as lactate and protons (H^+). Such information would also be able to develop improved understanding of transitions between lipid to carbohydrate catabolism, and from steady state to non-steady state exercise.

Therefore, the purpose of this study was to develop a new model to quantify the motor unit by motor unit increments that occur for measures of whole muscle kinetics and kinematics. More specifically, the model would compute the motor unit by motor unit incremental changes in contractile velocity, force, and power with increasing motor unit recruitment, and repeat this across four different categories of motor unit genetic expression.

Methods

A possible explanation for the sustained reliance on the "Black Box" model of muscle contraction in physiological and biochemical research, which remains to current times, is that there remains no methodology available to directly measure changes in motor unit recruitment within in-vitro animal models, or in-vivo human models of muscle contraction. This prevents knowledge of when motor unit recruitment transitions across different motor unit categories, and how each recruited motor unit contributes to contractile velocity, force, and power. Consequently, the initial phase of this research was to develop illustrative versions of the "Black Box" model (Figure 1) and a newly developed motor unit derived model of muscle contractile force and power (Figure 2).

The initial stage of the methods and model development was to read past research of human single skeletal muscle fibre contractile and metabolic function, and fibre type categorization using myosin heavy chain electrophoresis. Based on this work, the main human muscle used in this research was the vastus lateralis (1,15,19-23).

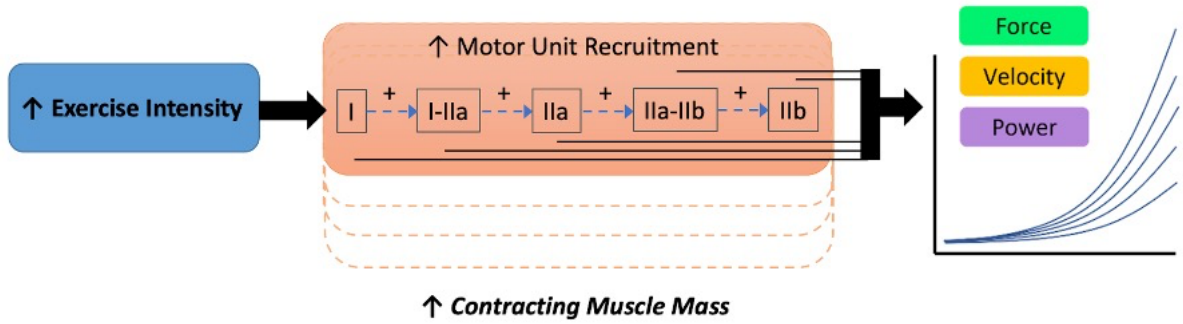

Figure 2: New model of the proposed representation for the development of contractile force, power, and velocity with increasing exercise intensity. Unlike the previous "Black Box" model, this accounts for the progressive motor unit recruitment controlling and determining the characteristics of muscle contraction.

Data for the size of this muscle and therefore the number and size of the muscle fibres was obtained from Lexell et al. (1) based on the dissection of entire vastus lateralis muscles from 5 cadavers of previously healthy and active young men. This work revealed an approximate number of muscle fibres of the vastus lateralis being 405,000. For the development of further data required for the model, this number differed slightly for each condition of motor unit expression due to accounting for a near normal distribution of the variability in motor unit sizes and fibre contractile function as explained in the next section. The muscle fibre typing based on ATPase histochemistry and myosin heavy chain expression was derived from the data and cited research presented in Table 1 (9,11,12,23,24). Slow twitch motor units were defined as comprising I and I-IIa categories (25), and the remainder were defined as fast twitch motor units.

To compute and model the contractile function and metabolism of the vastus lateralis there was a need to establish the fibre numbers per motor unit for each fibre type category. As there is no evidence of these values from research of human muscle, these were assumed to be 100, 120, 140, 160 and 180 fibres·unit^{-1} for the previously explained and reported (Table 1 and 2) sequence, respectively.

Based on the research of Bottinelli et al. (9) and Bottinelli (11), there is variability within the contractile and metabolic parameters of each of the fibre types. This was assumed to represent a near normal distribution having a range spanning ±15% of the mean (Figure 3). This distribution was applied to the motor unit muscle fibres and force variables for computations within the model.

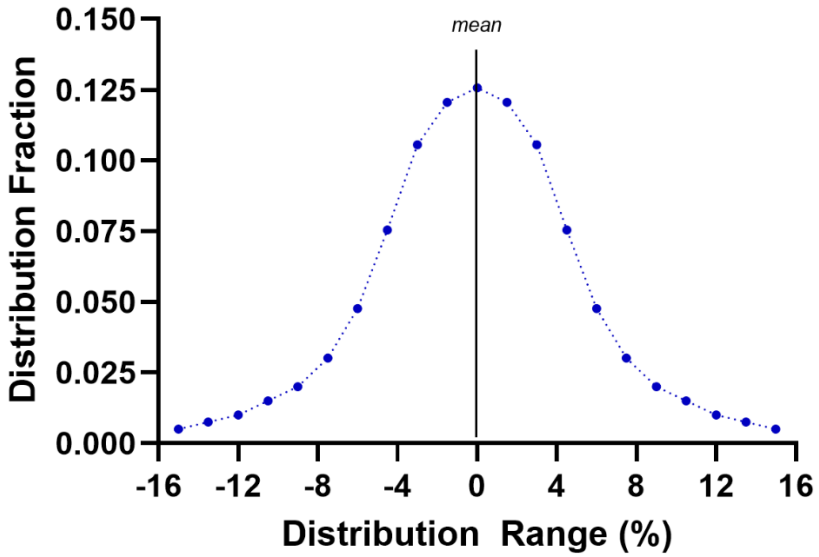

Figure 3: Visual representation of the near normal distribution fractional values for ±15% of the distribution range of motor unit size (fibres·unit^{-1}). See Methods for further details.

Single fibre muscle contractile force from the vastus lateralis were initially derived from the data of Bottinelli et al. (9). However, subsequent calculations within the model revealed errors in this data as calculations of whole muscle contractile force and power were too high compared to reasonable estimates of force generation from one muscle. Consequently, data from other studies were obtained. The results from Krivickas et al. (12) were retrieved and inserted into the initial spreadsheet program for calculations. The methodology of Bottinelli et al. (9) and Krivickas et al. (12) were similar in that they quantified single fibre contractile force during isotonic contractions and expressed force relative to the peak isometric force at 12 ˚C. This data was temperature corrected to 21 ˚C by a factor of 2, which was the highest temperature able to be researched prior to instability in the muscle fibre preparations (9,12). Furthermore, Bottinelli reported no further increases in contractile force for temperature increases above 15 ˚C (9). Temperature corrected contractile force data from Krivickas et

al. (12) produced more reasonable results based on comparisons to in-vivo quadriceps contractile force. However, Krivickas et al. (12) only studied single fibre contractile properties for type I and IIa muscle fibres. To provide a range of contractile force data across the five categories of motor units, increments in force were applied based on the relative force range of the data from Bottinelli et al. (9). This resulted in the data presented in Table 2 based on an increment in relative force of 0.15 per unit category from type I (factor of 1) to IIb fibres (factor of 1.6).

Table 2: Variables retrieved and calculated from prior research for contractile features of motor unit types (see text).

Type	Fibres ($\#\cdot unit^{-1}$)	Force (mN)	Velocity ($mm\cdot s^{-1}$)	Shortening^ (mm)	Time (s)	Power ($Nm\cdot s^{-1}$)	Power^ ($Nm\cdot cont'n^{-1}$)
I	100	0.4388	58.41	27.5	0.471	2.53E-5	5.38E-5
I-IIa	120	0.5046	117.56	27.5	0.234	5.93E-5	2.54E-4
IIa	140	0.5704	132.30	27.5	0.208	7.55E-5	3.63E-4
IIab	160	0.6362	172.47	27.5	0.160	1.10E-4	6.88E-4
IIb	180	0.7020	236.97	27.5	0.116	1.66E-4	1.43E-3

^per contraction duration and distance; force, velocity, time and power data are corrected for muscle temperature from 12 to 21 °C (see text)

Computational Features Of The LabVIEW Program

The contractile features of the vastus lateralis for different intensities and therefore motor unit recruitment was computed through custom developed software (LabVIEW, National Instruments, Austin, Texas USA). A flow diagram of the features involved in the development of the computational model is presented in Figure 4.

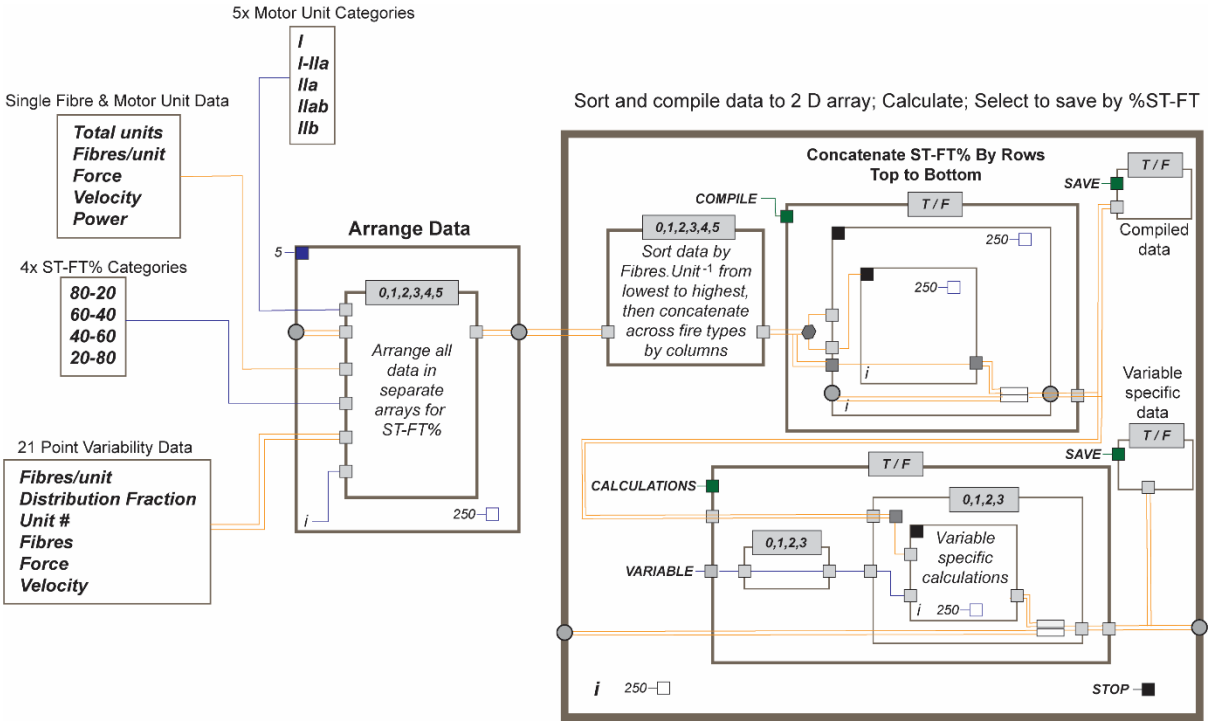

Figure 4: Visual representation of a thematic summary of the LabVIEW programming of the computational model.

The development of the computational model during programming was completed in two phases. Phase 1 involved the application of pertinent data from Tables 1 and 2 (fibres per unit, contractile velocity, contractile force, and contractile power) for each of the five motor unit categories identified by Bottinelli et al. (9) and later modified by the data of Krivickas et al. (12). The motor unit sizes across the five categories were assumed to be 100, 120, 140, 160, and 180 fibres·unit^{-1}, respectively. The ±15% distribution range (Figure 3) was applied to motor unit size, fibre contractile force, and fibre contractile velocity based on a 21-point data range, and data were organized in a commercial spreadsheet program (Microsoft Excel™, 2022). Computations were completed based on data adhering to results for total muscle fibres being as close as possible to the total muscle fibres of the vastus lateralis (405,000) as presented in Table 3. It was impossible to have this total muscle fibre value be a constant due to the constraints imposed by the computed numbers of motor units within the ±15% range and for conditions of genetic expression of slow to fast twitch motor units being 80-20, 60-40, 40-60, and 20-80%, respectively. An example of these preliminary data sets is presented in Table 4 for the muscle fibres of type I motor units for the 80-20% ST-FT.

Table 3: Morphological and bioenergetic features of the vastus lateralis.

Variables	Data	Source(s)
Total muscle fibres	405,000	25
Fibre length (mm)	83	21
Fractional contraction shortening	0.2989	21
Absolute contraction shortening (mm)	27.5	21
Fibre diameter (um)	95	3, 4, 17, 30
Fibre cross sectional area (um^2)	5,000	3, 4, 17, 30
Fibre angle (˚)	18	21
In-vivo efficiency of free energy transfer (fractional)	0.4	19

Phase 1 Mathematical Computations

The spreadsheet data sets of the distributions of motor unit types for specific genetic expressions of ST to FT proportions that were imported into the model initially involved a computation for determining the numeric distribution of muscle fibres·motor unit^{-1} (fMU) based on a ±15% range from the pre-determined mean (mFU) spanning a 21-point distribution (Table 4). The computation is presented in Equation 1 and was applied to each 21 numeric constants (k) (0-20).

$$fMU = mFU - \left((mFU * 0.15) + \left(k * \frac{(2 * 0.15) * mFU}{20}\right)\right)$$

Equation 1

Equation 1 was then applied to the fractional distribution resulting from Figure 3 to calculate the real fibre numbers per motor unit (nMU) based on the product of the fraction coefficient (f) and total motor units ($totMU$) for each of the 21-point distribution as shown in Equation 2.

$$nMU = f * totMU$$

Equation 2

The total fibres from each motor unit variant ($totF$) was calculated by the product of fMU and nMU as shown in Equation 3.

$$totF = fMU * nMU$$

Equation 3

Once the total motor unit and fibres·motor unit^{-1} numbers were known across the 21-point ±15% distribution, calculations of fibre and motor unit forces, velocities and powers could be calculated based on known data (constants) for these variables from the prior research of single muscle fibres from each fibre type (motor unit) category.

Force per muscle fibre (F) was calculated by simply replacing the mFU of Equation 1 with the force constant (k_F) expressed as milli-Newtons (mN) as shown in Equation 4.

$$F = k_F - \left((k_F * 0.15) + \left(k * \frac{(2 * 0.15) * k_F}{20}\right)\right)$$

Equation 4

The same principle of the F per muscle fibre calculation modification of Equation 1 was applied to velocity (v; mm·s^{-1}) using the velocity constant (k_v) as shown in Equation 5.

$$v = k_v - \left((k_v * 0.15) + \left(k * \frac{(2 * 0.15) * k_v}{20}\right)\right)$$

Equation 5

Power per muscle fibre (P) was calculated by the product of F and v, further corrected to Nm·s^{-1} as shown in Equation 6.

$$P = {}^{(F * v)}/_{1{,}000{,}000}$$

Equation 6

The muscle fibre F and P data needed to be converted to cumulative values representing the motor unit based on the number of muscle fibres per motor unit numbers in each of the 21-point distributions conditions. This was a simple computation for cumulative motor unit F (F_{mu}) based on the product of previously calculated data. For F_{mu} this was the product of fMU, nMU and F as shown in Equation 7.

$$F_{mu} = fMU * nMU * F$$

Equation 7

A similar computation for cumulative P (P_c) was based on the product of v and F_c as shown in Equation 8.

$P_c = v * F_c$

Equation 8

These calculations were repeated across the different fibre types (motor units) for each of the four genetic expression categories within the spreadsheet program. Once again, see Table 4 for a data set example.

Table 4: The preliminary data sets for the muscle fibres of type I motor units for the 80-20% ST-FT. * calculated from the sum of cumF x Vel (accounts for the number of real motor units).

I units =	#	fibres #/unit	Fraction	real # units	Fibres #	Force (mN)	Vel ($mm \cdot s^{-1}$)	Fibre Power ($Nm \cdot s^{-1}$)	cF (mN)	cPower ($Nm \cdot s^{-1}$)
2272	0	85	0.00500	11	966	0.3730	49.65	0.000018518	360.15	0.017880882
Fibres/unit=	1	87	0.0075	17	1474	0.3796	50.52	0.000019177	559.46	0.028266481
100	2	88	0.01	23	1999	0.3861	51.40	0.000019848	772.04	0.039683518
Half range %	3	90	0.015	34	3050	0.3927	52.28	0.000020531	1197.88	0.062621363
15	4	91	0.0225	51	4652	0.3993	53.15	0.000021224	1857.55	0.098734481
	5	93	0.03	68	6305	0.4059	54.03	0.000021930	2559.06	0.138263837
Tot Fibres =	6	94	0.0475	108	10144	0.4125	54.91	0.000022647	4184.31	0.229741431
227208.52	7	96	0.075	170	16273	0.4191	55.78	0.000023375	6819.35	0.380393888
	8	97	0.105	239	23140	0.4256	56.66	0.000024116	9849.35	0.558041701
Unit Factor	9	99	0.12	273	26855	0.4322	57.53	0.000024867	11607.23	0.667808726
2272	**10**	**100**	**0.125**	**284**	**28400**	**0.4388**	**58.41**	0.000025630	**12461.92**	**0.727900747**
	11	102	0.12	273	27673	0.4454	59.29	0.000026405	12325.04	0.730704068
Vel ($mm \cdot s^{-1}$)	12	103	0.105	239	24572	0.4520	60.16	0.000027191	11105.51	0.668133312
58.41	13	105	0.075	170	17807	0.4585	61.04	0.000027989	8165.24	0.498393405
	14	106	0.0475	108	11440	0.4651	61.91	0.000028798	5320.84	0.329437746
Force (mN)	15	108	0.03	68	7327	0.4717	62.79	0.000029619	3456.31	0.217024518
0.4386	16	109	0.0225	51	5572	0.4783	63.67	0.000030451	2665.08	0.169677464

	17	111	0.015	34	3766	0.4849	64.54	0.000031295	1825.96	0.117852892
	18	112	0.01	23	2545	0.4915	65.42	0.000032151	1250.58	0.081811851
	19	114	0.0075	17	1943	0.4980	66.30	0.000033018	967.47	0.064138676
	20	115	0.005	11	1306	0.5046	67.17	0.000033896	659.24	0.044281842
Mean		**100.02**				**0.4388**	**58.41**	0.000025842		
Sum			**1.0**	**2272**	**227,209**				**99969.57**	**5.871**

Phase 2 Mathematical Computations

Phase 2 involved the importing of the data sets into LabVIEW™ (National Instruments, Austin, TX) as summarized in Figure 4. The following simple mathematical procedures then occurred based on user operation and selection. A detailed description and the related equations follow.

The data sets for all motor unit categories of each percent expression of slow to fast twitch motor units were entered into the computational program from which further programming features directed future computations. As the progression of motor unit size increased from type I through to type IIb, data for each motor unit type was collated in sequential rows of a two-dimensional data array. This was completed separately for each genetic expression of slow to fast twitch motor units.

Each two-dimensional data array was then compiled to account for the changing motor unit sizes across the ±15% distribution range within each motor unit category. For example (see Table 4), the initial motor unit of the type I category (which would be the first recruited in all contractions of the vastus lateralis) had 85 fibres·unit^{-1}, a distribution representation of 0.005, which equated to 11 of the 2272 type I motor units within the 80-20% genetic expression of slow to fast twitch motor units, and represented 966 muscle fibres that each had a force of 0.373 mN, a contractile velocity of 49.65 mm·s^{-1} and a power of 1.8518 Nm·s^{-1}·E^{-5}. Based on the summed force of all the type-I motor units contracting at an average velocity across the motor units, summed power equated to 5.871 Nm·s^{-1} (1 Nm·s^{-1} = 1 Watt). To ensure the ability to model the recruitment of individual motor units the programming of the compilation used the number of motor units of a given fibres·unit^{-1}size to duplicate the contractile force and velocity data of each data array row entry. This had to be repeated for the 21 levels of the near normal distribution for all motor unit categories and genetic expressions. The end-result was a data array where each row represented a different motor unit.

The overlap of motor unit recruitment between motor unit categories required added custom software to identify the type of motor unit that was recruited in the sequential order. This first required the

insertion of numeric labels for each motor unit category for every row of the total muscle motor units of the vastus lateralis, as follows; 1=I, 2=I-IIa, 3=IIa, 4=IIab, and 5=IIb. This labelling column of the array was then used to programmatically sequence and count the number of motor units recruited from all categories for increments in recruitment of 20, 40, 60, 80, 100%. The final variables calculated for the partial recruitment conditions were the number of motor units recruited and the percent recruitment for all motor unit categories across each of the four genetic expressions of muscle motor unit proportions for the previous increments in motor unit recruitment.

The sequential recruitment of motor units was calculated for each individual increment in motor unit recruitment, which then enabled specific conditions of % motor unit recruitment as explained above. The average of all recruited motor unit contractile velocities for each recruitment condition was used to quantify final contractile velocity, force and power for the muscle contraction, as described next.

For velocity, each motor unit row was incrementally summed (v_s) then averaged, where each row was an average of the rows prior and inclusive of the current row, where the averaged velocity represented the contractile velocity of the total incremental motor unit pool.

$$v_{mean} = \left(\sum_{k=n+1}^{n} \binom{n}{k} v_s\right) \Big/ n$$

Equation 9

For force, each motor unit was sequentially summed, row by row producing an equal row number of incremental summed F_{mu} data (F_s;Equation 10), which in turn was repeated for each of the four percent slow to fast twitch genetic expressions.

$$F_s = \sum_{k=n+1}^{n} \binom{n}{k} F_{mu}$$

Equation 10

For power (P), F was converted from mN to N, and v was converted from mm·s^{-1} to m·s^{-1}. Power (Nm·s^{-1}) was then the simple product of each incremental row of F_s and v_{mean} (P_s;Equation 11), which in turn was repeated for each of the four percent slow to fast twitch genetic expressions.

$$P_s = \sum_{k=n+1}^{n} \binom{n}{k} (F_s \times v_{mean})$$

Equation 11

Final data for velocity, force and power were each saved in separate .txt files representing the incremental changes across the motor units based on recruitment determined by motor unit size.

Data Processing

To present the data for the change in force, velocity, and power for sequential motor unit recruitment of vastus lateralis, non-linear curve fitting was employed (GraphPad Prism version 8.0.0 for Windows, GraphPad Software, San Diego, California USA) as follows: For contractile force; 20-80 = polynomial 2nd order; 40-60 = polynomial 3rd order; 60-40 = polynomial 4th order; 80-20 = polynomial 5th order. For contractile power; 20-80 = polynomial 3rd order; 40-60 = polynomial 4th order; 60-40 = polynomial 5th order; 80-20 = polynomial 6th order. For velocity the resulting data profile was too complex for curve fitting and data were left as a sequence of data points.

Results

In addition to the data retrieved from prior research (Tables 1 and 2) as explained in Methods, an example of the added data used within the programming of the model were presented in Table 4. Such data were also calculated for the added four motor unit categories, and all repeated for the added motor unit expressions of 60-40, 40-60, and 20-80 ST-FT%. Thus, this preliminary data that was used within the model amounted to 5 data sets of 11 columns and 21 rows of data for each of the 4 ST-FT% motor unit expressions. This equated to 4,620 data points.

Data resulting from the model for each motor unit type of each motor unit proportionality category are presented in Tables 5-8. Total fibres for the vastus lateralis differed slightly for each proportionality category due to constraints caused by the different fibres per unit features across the motor unit categories. Best efforts were adhered to in developing this data to keep these numbers as close as possible to 405,000. This variability is also seen in the total percent results for each expression of motor unit proportionality.

Table 5: Data Development for 80-20 Proportionality

	Type	Mean Fibre Number·unit^{-1}	Unit Number	Total Fibres	% Total	% Type	Total Fibres	Total %
ST	**I**	100	2270	227562	56	69.79		
	I-IIa	120	821	98520	24	30.21	326082	80.33
FT	**IIa**	140	170	24102	6	30.19		
	IIab	160	95	15040	4	18.84		
	IIb	180	226	40687	10	50.97	79829	19.67
	SUM		**3582**	**405911**	**100**			**100**

Table 6: Data Development for 60-40 Proportionality

	Type	Mean Fibre Number·unit^{-1}	Unit Number	Total Fibres	% Total	% Type	Total Fibres	Total %
ST	**I**	100	1716	172025	42	70.60		
	I-IIa	120	597	71640	18	29.40	243665	60.10
FT	**IIa**	140	359	50300	12	31.10		
	IIab	160	151	24160	6	14.94		
	IIb	180	485	87300	22	53.97	161760	39.90
	SUM		**3308**	**405425**	**100**			**100**

Table 7: Data Development for 40-60 Proportionality

	Type	Mean Fibre Number·unit^{-1}	Unit Number	Total Fibres	% Total	% Type	Total Fibres	Total %
ST	**I**	100	1136	113600	28	69.78		
	I-IIa	120	412	49200	12	30.22	162800	40.30
FT	**IIa**	140	542	75580	19	31.34		
	IIab	160	279	44640	11	18.51		
	IIb	180	672	120960	30	50.15	241180	59.70
	SUM		**3041**	**403980**	**100**			**100**

Table 8: Data Development for 20-80 Proportionality

	Type	Mean Fibre Number·unit^{-1}	Unit Number	Total Fibres	% Total	% Type	Total Fibres	Total %
ST	**I**	100	562	56200	14	69.04		
	I-IIa	120	210	25200	6	30.96	81400	20.15
FT	**IIa**	140	680	95200	24	29.51		
	IIab	160	375	60000	15	18.60		
	IIb	180	930	167400	41	51.89	322600	79.85
	SUM		**2757**	**404000**	**100**			**100**

The change in contractile force, velocity, and power with sequential increases in motor unit recruitment, for each of the four expressions of motor unit proportions, are presented in Figures 5a,b,c. Note that the total number of motor units differed between the motor unit expression categories due to the near constant total number of muscle fibres and the larger number of muscle fibres per unit as you progress from Type I to Type IIb.

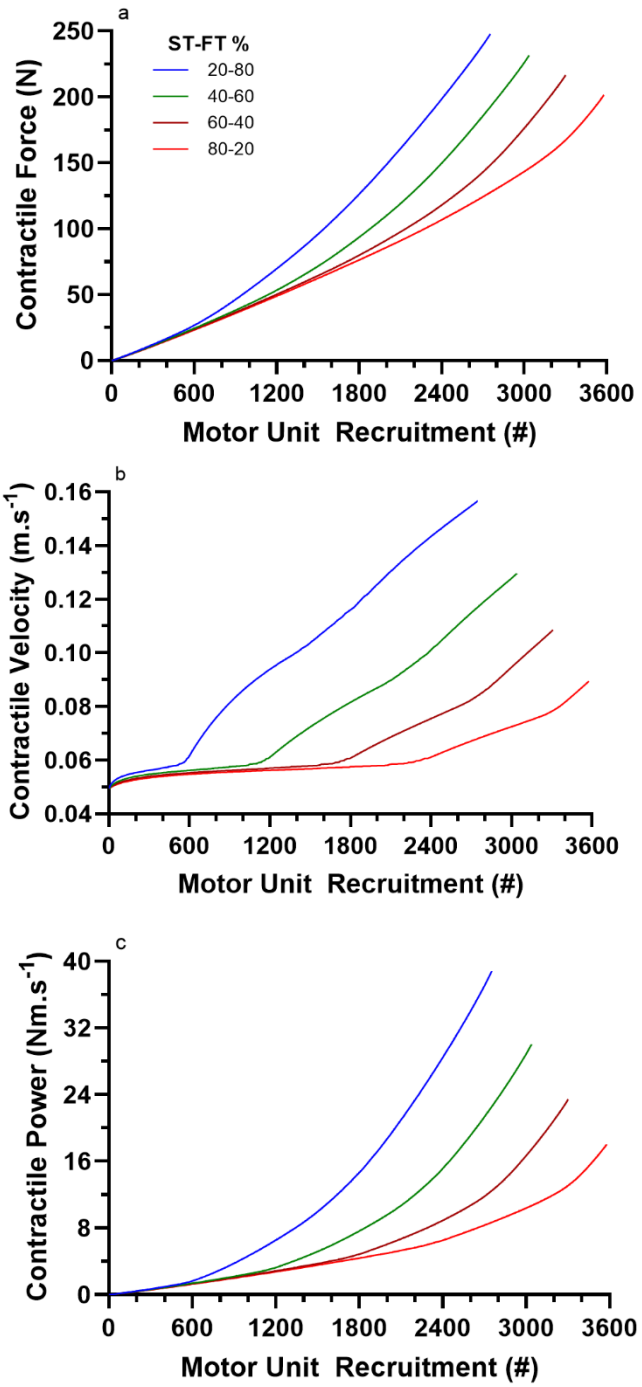

Fig. 5: Stack plot of the results from the model for the sequential motor unit recruitment across the entire motor unit pool of the vastus lateralis. a) Contractile Force, b) Contractile Velocity, c) Contractile Power. Note the motor unit proportion categories represented by the different lines (see Figure a legend).

Table 9: The total and individual motor unit type recruitment for the different proportion conditions, and their relative recruitment in increments of 20%.

	Recruited Units			I			I-IIa			IIa			IIab			IIb			Velocit	Force	Power
Proportion	**#**	**%**	**Fibres**	**#**	**%**	**Fibres**	**#**	**%**	**Fibres**	**#**	**%**	**Fibres**	**#**	**%**	**Fibres**	**#**	**%**	**Fibres**	**$m \cdot s^{-1}$**	**N**	**Watts**
20% recruitment																					
80-20	717	20	67733	717	31.5	67733	0	0	0	0	0	0	0	0	0	0	0	0	0.055	28.065	1.545
60-40	662	20	63065	662	38.5	63065	0	0	0	0	0	0	0	0	0	0	0	0	0.0554	26.334	1.461
40-60	608	20	58662	608	53.5	58662	0	0	0	0	0	0	0	0	0	0	0	0	0.0562	24.805	1.394
20-80	551	20	55038	541	96.2	53977	10	4.7	1061	0	0	0	0	0	0	0	0	0	0.0589	24.103	1.421
40% recruitment																					
80-20	143	40	13936	143	63.1	13936	0	0	0	0	0	0	0	0	0	0	0	0	0.056	59.400	3.365
60-40	132	40	12994	132	76.9	12963	3	0.5	306	0	0	0	0	0	0	0	0	0	0.0573	55.953	3.207
40-60	121	40	12279	113	100	11388	80	19.	8915	0	0	0	0	0	0	0	0	0	0.0617	54.286	3.351
20-80	110	40	12588	562	100	56335	210	100	25200	32	48.	43668	5	1.3	686	0	0	0	0.0902	61.826	5.583
60% recruitment																					
80-20	215	60	21410	212	93.3	21093	30	3.6	3164	0	0	0	0	0	0	0	0	0	0.059	93.467	5.477
60-40	198	60	20286	171	100	17202	267	44.	30599	2	0.5	238	0	0	0	0	0	0	0.0657	90.592	5.953
40-60	182	60	20038	113	100	11388	410	100	49200	27	50.	36888	3	1.0	412	0	0	0	0.0822	95.471	7.848

20-80	165	60	20785	562	100	56335	210	100	25200	67	99.	94317	18	49.	28723	21	2.25	3279	0.110	110.99	12.210
80% recruitment																					
80-20	286	80	29742	227	100	22756	592	72.	69378	4	2.3	486	0	0	0	0	0	0	0.070	134.62	9.441
60-40	264	80	22535	171	100	17202	597	100	7164	32	90.	44888	9	5.9	1280	0	0	0	0.0809	138.05	11.178
40-60	243	80	29388	113	100	11388	410	100	49200	54	100	75896	25	89.	39747	92	13.6	15163	0.1024	153.24	15.702
20-80	220	80	30162	562	100	56335	210	100	25200	67	100	94800	36	97.	58370	39	41.8	66917	0.1352	173.66	23.379
100% recruitment																					
80-20	358	10	40591	227	100	22756	821	100	98520	17	100	24102	94	100	15040	22	100	40687	0.090	202.01	18.136
60-40	330	10	40541	171	100	17202	597	100	7164	35	100	50271	15	100	24160	48	100	87315	0.1085	217.57	23.607
40-60	303	10	40459	113	100	11388	410	100	49200	54	100	75896	27	100	44640	67	100	12098	0.1295	232.04	30.059
20-80	275	10	40412	562	100	56335	210	100	25200	67	100	94800	37	100	60000	93	100	16778	0.1569	248.14	38.957

Data for the progressive sequential motor unit recruitment from the different motor unit categories for 20% increments in motor unit recruitment are presented in Table 9, along with resulting data for contractile force, power, and velocity. As with the complete data presented in Figure 5a,b,c, note the non-linear increase in force, power, and velocity with increases in motor unit recruitment, and for increased fast twitch motor unit proportionality.

Discussion

Overview

This study proposed and developed a model for the influence of the size principle of progressive motor unit recruitment on the development of contractile velocity, force, and power of the human vastus lateralis muscle. Prior to this study, a simple "Black Box" model (entire and homogenous muscle contractile function) of muscle contractile function has remained the sole conceptual foundation for understanding the biochemistry and mechanics of force generation in skeletal muscle. Textbooks of Medical Physiology are a prime example, where the most widely used resource continues to refer to skeletal muscle contraction in the context of a whole muscle and not the sequential recruitment of individual motor units based on the "Size" and "All Or None" principles (26).

Of added concern is that scientific progress on this topic remains constrained due to the inability to measure motor unit recruitment in humans during exercise and isolate contributions from the muscle fibres of these motor units to contractile force, velocity, and power. The results of this study revealed that the modelling of individual motor unit contributions to contractile function in a single muscle (vastus lateralis) can be accomplished using data from prior research of single skeletal muscle fibre physiology. Added results revealed that the profiles of contractile velocity, force, and power are non-linear across the range of motor unit recruitment. Such non-linearity is explained by the progressive increase in motor unit size (fibres·unit^{-1}) and the related increases in force increment with increasing fast twitch motor unit recruitment.

These findings are interesting based on their extension to interpretations from prior research that is largely constrained by the small sampling of skeletal muscle through muscle biopsy, and the related methodology involving histological staining and/or myosin heavy-chain composition. How the results from this study both support and extend this prior research will be the focus of the rest of the discussion.

Brief History Of The Development of the Size Principle of Motor Unit Recruitment

In 1938, Denny-Brown and Pennybacker (27) observed the orderly recruitment of skeletal muscle motor units (cumulative activation) and in 1957 Henneman (28) proposed a “Size Principle" mechanism of motor unit recruitment. The word “size” in this context was defined as the cumulative surface area of the motor neuron soma and its dendrites. This early definition by Henneman stated:

“*The amount of excitatory input required to discharge a motoneuron, the energy it transmits as impulses, the number of fibres it supplies, the contractile properties of the motor unit it innervates, its mean rate of firing and even its rate of protein synthesis are all closely correlated with its size. This set of experimental facts and interrelations has been called the ‘size principle’.*”

Further studies have justified inclusions to the parameters of the size principle, such as muscle fibre conduction velocity identified by Andreassen and Arendt-Nielsen (29) being consistent with gradual recruitment of larger motor units with larger twitch tension and higher muscle fibre conduction velocity. Similar results for the cat gastrocnemius muscle were reported earlier by Burke and Tsairis (30). Continued research has studied and challenged the validity of the size principle (31-35) yet it has remained one of the most fundamental principles in the organisation of motor unit behaviour to current time (36).

As there were no prior data on the nerve soma characteristics of human motor units, we had to base differences in motor unit size solely on the number of muscle fibres per unit. Given that these numbers are unknown for human skeletal muscle we assumed differences in fibres per unit ranging from means of 100 to 180 fibres·unit^{-1}. As shown in Figure 5a-c, the results indicated a curvilinear increase in contractile force and power with increases in motor unit recruitment. With a larger number

of muscle fibres per motor unit in the fast twitch categories, this result was anticipated. Data of the progressive recruitment in 20% increments for the different proportions of the different motor unit types is presented in Table 9. The data of Table 9 are important because they show the gradual increase in the motor unit categories with 20% increments in recruited motor units for the four different relative expressions of slow twitch to fast twitch categories. For example, note the delayed recruitment of fast twitch motor unit categories (IIa, IIab, IIb) until intensities >60% of total motor unit recruitment. If we focus on the 80-20% proportionality, the total number of recruited fibres increased from 67,733 to 405,911. The recruitment of type I motor units increased from 31.59 to 63.13, 93.39 and 100% for motor unit recruitment totals of 20, 40, 60, 80%, respectively.

Knowledge Gained From Histological Staining of Skeletal Muscle Fibres

Despite the "Black Box" representation of skeletal muscle, advances in technology have allowed analyses of individual skeletal muscle fibre structure and function. This was necessary to understand the potential variability of the typical fibre characteristics (e.g., slow twitch oxidative fibres having higher mitochondrial density and relative fatigue resistance characteristics; fast glycolytic being low in mitochondrial content, high force, and easily fatigued). Though to current time there is no method to reveal which muscle fibres sampled from human whole muscles are from which specific motor unit. Nevertheless, analyses of muscle fibre type contributions to muscle involvement and metabolism during exercise have been completed through ATPase and periodic acid-schiff base (PAS) staining of serial sections of biopsy samples.

Historical Studies of Fibre Type Specific Involvement With Exercise Intensity

In an early study (37), the depletion pattern of glycogen was examined after cycling at varying intensities. Different pedalling rates were used ranging from 30-120 rev·min^{-1}, reaching work intensities of 30-150% of VO_2max, and sustaining from several hours to 1 min. PAS staining of skeletal muscle fibres indicated an increased level of glycogen utilisation with increasing exercise intensity. The fibre-specific results indirectly indicated the metabolic consequence of progressive motor unit recruitment with increasing intensity. Reduced PAS straining at pedalling rates inducing

30-100% of VO_2max revealed the slow twitch, high oxidative fibres to be the first to deplete glycogen, and as intensity increase up to 150% VO_2max, the fast twitch fibres progressively depleted glycogen. Whole muscle biopsy biochemical assay 3 hrs post low intensity exercise indicated large amounts of glycogen remained, and based on the serial section PAS staining, this was predominately in the fast twitch fibres. It was also found that the pattern of such depletion was unaffected by the pedalling rate (i.e., total force on each push), indirectly supporting the size principle of motor unit recruitment.

Similarly, Vollestad et al. (38) used exhaustive bicycle exercise (i.e., prolonged maintenance of 75% of VO_2max, at a constant 70 rev·min^{-1} pedalling rate) to study the glycogen depletion patterns in type I, IIa, IIab and IIb fibres. Total glycogen content of 29 biopsies of the vastus lateralis were compared to average PAS stain intensity in sections from the same samples. They found a successive glycogen depletion occurring in the fibres following the simultaneous recruitment of type I and IIa, with type IIab following, then finally IIb. Similar results were reported by De Bock et al. (39).

Despite the extensive information gained from such methods, the limitation of sample size remains as does the inability to know which fibres are from which motor units within the categories revealed through ATPase staining. Interpretation of the muscle activity and resulting fibre type differences from muscle biopsies relies on the assumption that the biopsy sample is an accurate representation of the fibre type distribution of the entire muscle. Lexell et al. (1) quantified the extent of biopsy sampling error in their study of the data obtained from cross sections of the vastus lateralis from young male individuals. The authors concluded that the large variability in the distribution of muscle fibres of different motor unit types within a whole muscle means a single biopsy is a poor estimator of fibre proportions. More specifically, there is a reduced sampling error in sampling over 150 fibres when more than three biopsies of a muscle are taken, with further reductions in sampling error with more biopsies per individual at varying depths within the muscle. Similarly, Nederveen et al. (40) highlighted a higher variation of fibre type distribution in the muscle cross sectional areas when less than 150 muscle fibres were quantified.

Models in Science

Within science, modelling can be used for a variety of reasons, with a core purpose being to apply current knowledge to conditions or questions that we may be unable to answer due to constraints in knowledge and/or instrumentation. Human physiology is an area that greatly relies on the projection of knowledge provided by such models.

"High order questions" as defined by Rosenblueth and Wiener (41) are very abstract and general questions in science and are not directly amenable to an experimental test. Instead, generalisations and numerous trivial experiments yield progress from data to predictions and vice versa. This can be done through material and formal models. Material being a complex system represented through another similar, yet simpler system, and formal being an idealised, simpler version of the original factual system. Therefore, models can provide the ability to replace a phenomenon in an unfamiliar field by one in a field the scientist is more knowledgeable and comfortable in, or they may enable the completion of experiments under more favourable conditions than required in the original system (41). However, a material model is considered unnecessary if it does not suggest any experiments whose results could not have been easily anticipated by the formal model alone. Additionally, a model does not represent progress if its structure is more complex and is less adaptable to experiment than the original system.

Comparison of Results to Prior Evidence of Muscle Contractile Function

The model-based novelty of this research makes it difficult to compare our results simply because this work has pioneered a new means to assess muscle contractile function. The approach taken in the use of a single muscle (vastus lateralis) is in stark contrast to the complexity of voluntary movement involving knee extension exercise as this reality involves the activation of numerous muscles that act in concert to cause knee extension. Nevertheless, the data from Table 9 presented forces ranging from 28 N (20% recruitment for 80-20 %ST-FT expression) to 248 N (100% recruitment for 20-80 %ST-FT expression). Bazzucchi et al. (42) compared *in-vivo* muscular contractile peak force differences of isometric elbow flexion and knee extension between young (20 to 31-year-olds) to older (68 to 76-

year-olds) healthy women. At 80% maximal voluntary contraction, the young women produced peak knee extension forces of 313.83 ± 69.25 N. Similarly, Thornley et al. (23) explored the influence of local tissue temperature on peak torque and time to fatigue during isometric knee extensions. Although concluded to be insignificant, the male participants in the study produced 70% maximum voluntary contractions with peak torque sitting around 207 ± 40 Nm. The peak *in vivo* force output measured in these studies is produced by multiple muscles acting on the movement of knee extension (i.e., the whole quadriceps group). Considering the single vastus lateralis muscle used in our study, the peak forces of 202 to 248 N compare favourably to prior research.

Similarly, peak contractile power as presented in Table 9 ranged from 1.5 (20% recruitment for 80-20 %ST-FT expression) to 38.9 Watts (100% recruitment for 20-80 %ST-FT expression) and is considerably lower than data measured in many studies involving *in vivo* multiple muscle contractions. However, being in-vivo and the product of force and velocity, both of which are greatly influenced by the multiple factors around full joint mechanics, power is expected to be much higher than the single muscle power generation. Complex movements, such as cycling, is a prime example. Elmer et al. (5) studied joint-specific power production during cycling and measured knee extension during maximal efforts to reach 232 ± 29 Watts despite knee flexion power becoming relatively more important during high-intensity cycling. Yet, once again our results only apply to a single contraction from the vastus lateralis without the added functional and mechanical advantages of added agonist muscle involvement, the moment arm with leverage providing torque, as well as the biomechanics of power being transferred through the body to the pedals.

Limitations Of The Model

The vastus lateralis muscle model used in this study involved one isolated muscle, while further ignoring the added increments in force that can result from the temporal summation of given motor units (as distinct from the summation from the recruitment of different motor units). Consequently, contractions generated exhibit the "All Or Nothing" principle, whereby the recruited motor units contracted maximally from a single neural stimulation so that the number and type of motor units recruited dictated the overall muscle's contractile profile. In addition, in being an isolated single

muscle model, the influence of musculoskeletal features such as the moment arm, external loads, fibre pennation angles, the lack of associated agonists and inhibition of antagonists, etc., were disregarded.

There were also limitations within the structure of the model. For example, the motor unit sizes (fibres·unit^{-1}) are unknown for humans and were generalised from prior animal research (see Table 2), and the size of the recruited fibres per motor unit were the sole feature that dictate the order of motor unit recruitment. This differs to in-vivo physiology where the size of the motor nerve cell body and its balance of stimulatory and inhibitory synapses predominantly influences the order of motor unit recruitment.

The classic human single muscle fibre research revealed considerable variability of muscle fibre structure and function within different motor unit categories (9,11,12,24). Based on this evidence, we assumed a consistent ±15% variability for the muscle fibres of each motor unit category for the variables: motor unit size, contractile force, and velocity.

The model computed the change in contractile velocity with increasing motor unit recruitment as a simple average of the contractile velocity of the muscle fibres contracting for the different conditions of motor unit recruitment. This differs from in-vivo conditions where the central nervous system requires increasing time to develop a motor unit recruitment profile as the number of motor units recruited increases, with added neural processing time for recruitment that progresses from slow twitch to fast twitch motor units.

Conclusions & Recommendations

In summary, this investigation highlighted the need for further research into the roles of skeletal muscle fibre types and the impact of their progressive recruitment during exercise. The developed model has provided an “abstraction” to the contractile functions of skeletal muscle, providing a new foundation for further modelling the biochemistry and energetics of skeletal muscle. Data from prior research of skeletal muscle fibre physiology ensured a level of accuracy to the computed results of progressive increases in motor unit size and the related increases in force increment with increasing fast twitch motor unit recruitment. Finally, the model has ascertained the relevance of transferring

data from single muscle fibre mechanics to whole muscle function while also providing insight into how such modelling can improve understanding of the mechanistic influences of motor unit recruitment at both the cellular and muscle level.

Researchers are encouraged to critically evaluate the model used in this research and to strive to make further improvements to ensure improved understanding of motor unit recruitment, and their outputs, across a diverse number of topics within physiology and metabolic biochemistry.

Acknowledgements

Feedback on manuscript content and data interpretation was provided by postgraduate students Bridgette O'Malley (PhD candidate) and Samuel Lewis Torrens (PhD candidate).

Reference List

1. Lexell J, Henriksson-Larsén K, Winblad B, Sjöström M. Distribution of different fiber types in human skeletal muscles: Effects of aging studied in whole muscle cross sections. Muscle & Nerve 1983;6:588–595. https://doi.org/10.1002/mus.880060809
2. Marcucci L, Reggiani C, Natali AN, Pavan PG. From single muscle fiber to whole muscle mechanics: a finite element model of a muscle bundle with fast and slow fibers. Biomechanics and Modeling in Mechanobiology 2017;16:1833–1843. https://doi.org/10.1007/s10237-017-0922-6
3. Spriet LL, Soderland K, Bergstrom M, Hultman E. Journal of Applied Physiology 1987;62:611-615. https://doi.org/10.1152/jappl.1987.62.2.611
4. Cheng EJ Brown IE Loeb GE. Virtual muscle: a computational approach to understanding the effects of muscle properties on motor control. J Neurosci Methods 2000;101:117-130. https://doi.org/10.1016/S0165-0270(00)00258-2
5. Elmer SJ, Barratt PR, Korff T, Martin JC. Joint-specific power production during submaximal and maximal cycling. Medicine and Science in Sports and Exercise 2011;43:1940–1947. https://doi.org/10.1249/MSS.0b013e31821b00c5
6. Hill AV. The heat of shortening and the dynamic constants of muscle. Proc R Soc Lond B Biol Sci 1938;126:136–195.
7. Brooke MH, Kaiser KK. Three human myosin ATPase systems and their importance in muscle pathology. Neurology 1970;20:404–405.
8. Schiaffino S, Reggiani C. Skeletal Muscle Fiber Types. In Hill JA, Olson EN (eds), Muscle: Fundamental Biology and Mechanisms of Disease 1st edn. 2012, Academic Press, Elsevier, London, pp. 855-867. https://doi.org/10.1016/B978-0-12-381510-1.00060-0
9. Bottinelli R, Canepari M, Pellegrino MA, Reggiani C. Force-velocity properties of human skeletal muscle fibres: myosin heavy chain isoform and temperature dependence. The Journal of Physiology 1996;495:573–586. https://doi.org/10.1113/jphysiol.1996.sp021617

10. Hawkins DA, Hull ML. An activation-recruitment scheme for use in muscle modeling. J Biomechanics 1992;25:1467-1476.
11. Bottinelli R. Functional heterogeneity of mammalian single muscle fibres: Do myosin isoforms tell the whole story? Pflügers Archiv 2001;443:6–17. https://doi.org/10.1007/s004240100700
12. Krivickas LS, Dorer DJ, Ochala J, Frontera WR. Relationship between force and size in human single muscle fibres: Muscle fibre size and force. Experimental Physiology 2011;96:539–547. https://doi.org/10.1113/expphysiol.2010.055269
13. Staron RS, Hagerman FC, Hikida RS, Murray TF, Hostler DP, Crill MT, Ragg KE, Toma K. Fiber Type Composition of the Vastus Lateralis Muscle of Young Men and Women. The Journal of Histochemistry and Cytochemistry 2000;48:623–629. https://doi.org/10.1177/002215540004800506
14. Henriksson-Larsen K, Wretling ML, Lorentzon R, Oberg L. Do muscle fibre size and fibre angulation correlate in pennated human muscles? European Journal of Applied Physiology and Occupational Physiology 1992;64:68–72. https://doi.org/10.1007/BF00376443
15. Gouzi F, Maury J, Molinari N, Pomiès P, Mercier J, Préfaut C, Hayot M. Reference values for vastus lateralis fiber size and type in healthy subjects over 40 years old: a systematic review and meta-analysis. Journal of Applied Physiology 2013;115:346–354. https://doi.org/10.1152/japplphysiol.01352.2012
16. Song D, Raphael G, Lan N, Loeb GE. Computationally efficient models of neuromuscular recruitment and mechanics. J Neural Eng 2008;5:175-184. https://doi.org/10.1088/1741-2560/5/2/008
17. Potvin JR, Fuglevand AJ A motor unit-based model of muscle fatigue. PLOS Comput Biol 13:e1005581. https://doi.org/10.1371/journal.pcbi.1005581
18. Fuglevand AJ, Winter DA, Patla AE. Models of recruitment and rate coding organization in motor-unit pools. J Neurophysiol 1993;70:2470-2488. https://doi.org/10.1152/jn.1993.70.6.2470
19. Brod GA, Geremia JM De Oliveira Melo M, Vaz MA, Loss JF. Vastus lateralis muscle architecture to estimate knee extension moment of older individuals. Motriz : Revista de Educação Física. Unesp 2015;21:428–435. https://doi.org/10.1590/S1980-65742015000400013

20. Edgerton VR, Smith J., Simpson DR. Muscle fibre type populations of human leg muscles. The Histochemical Journal 1975;7:259–266. https://doi.org/10.1007/BF01003594
21. Horwath O, Envall H, Röja J, Emanuelsson EB, Sanz G, Ekblom B, Apró W, Moberg M. Variability in vastus lateralis fiber type distribution, fiber size, and myonuclear content along and between the legs. Journal of Applied Physiology 2021;131:158–173. https://doi.org/10.1152/japplphysiol.00053.2021
22. Pernus F, Erzen I. Fibre size, atrophy, and hypertrophy factors in vastus lateralis muscle from 18- to 29-year-old men. Journal of the Neurological Sciences 1994;121:194–202. https://doi.org/10.1016/0022-510X(94)90352-2
23. Thornley LJ, Maxwell NS, Cheung SS. Local tissue temperature effects on peak torque and muscular endurance during isometric knee extension. European Journal of Applied Physiology 2003;90:588–594. https://doi.org/10.1007/s00421-003-0927-y
24. Medler S. Mixing it up: The biological significance of hybrid skeletal muscle fibers. Journal of Experimental Biology 2019;22:23. https://doi.org/10.1242/jeb.200832
25. Westwood FR, Bigley A, Randall K, Marsden AM, Scott RC. Statin-induced muscle necrosis in the rat: distribution, development, and fibre selectivity. Toxicologic Pathology 2005;33:246–257. https://doi.org/10.1080/01926230590908213
26. Hall JE. Guyton & Hall Physiology Review (3rd ed.). 2015, Elsevier Health Sciences, London.
27. Denny-Brown D, Pennybacker JB. Fibrillation and Fasciculation in Voluntary Muscle. Brain 1938;61:311–312. https://doi.org/10.1093/brain/61.3.311
28. Henneman E. Relation between size of neurons and their susceptibility to discharge. Science 1957;126:1345–1347. https://doi.org/10.1126/science.126.3287.1345
29. Andreassen S, Arendt-Nielsen L. Muscle fibre conduction velocity in motor units of the human anterior tibial muscle: a new size principle parameter. The Journal of Physiology 1987;391:561–571. https://doi.org/10.1113/jphysiol.1987.sp016756
30. Burke RE, Tsairis P. Anatomy and innervation ratios in motor units of cat gastrocnemius. The Journal of Physiology 1973;234:749–765. https://doi.org/10.1113/jphysiol.1973.sp010370

31. Cope T, Pinter MJ. The Size Principle: Still Working After All These Years. Physiology 1995;10:280-286. https://doi.org/10.1152/physiologyonline.1995.10.6.280
32. Fling BW, Knight CA, Kamen G. Relationships between motor unit size and recruitment threshold in older adults: implications for size principle. Experimental Brain Research 2009;197:125–133. https://doi.org/10.1007/s00221-009-1898-y
33. Gordon T, Thomas, CK, Munson JB, Stein RB. The resilience of the size principle in the organization of motor unit properties in normal and reinnervated adult skeletal muscles. Canadian Journal of Physiology and Pharmacology 2004;82:645–661. https://doi.org/10.1139/y04-081
34. Holt NC, Wakeling JM, Biewener AA. The effect of fast and slow motor unit activation on whole-muscle mechanical performance: the size principle may not pose a mechanical paradox. Proceedings of the Royal Society. B, Biological Sciences 2014;281:1-6. https://doi.org/10.1098/rspb.2014.0002
35. Mendell LM. The size principle: a rule describing the recruitment of motoneurons. Journal of Neurophysiology 2005;93:3024–3026. https://doi.org/10.1152/classicessays.00025.2005
36. Enoka RM, Stuart DG. Henneman's "size principle": current issues. Trends in Neurosciences 1984;7:226–228. https://doi.org/10.1016/S0166-2236(84)80210-6
37. Gollnick PD, Piehl K, Saltin B. Selective glycogen depletion pattern in human muscle fibres after exercise of varying intensity and at varying pedalling rates. The Journal of Physiology 1974;241:45–57. https://doi.org/10.1113/jphysiol.1974.sp010639
38. Vøllestad NK, Vaage O, Hermansen L. Muscle glycogen depletion patterns in type I and subgroups of type II fibres during prolonged severe exercise in man. Acta Physiologica Scandinavica 1984;122:433–441. https://doi.org/10.1111/j.1748-1716.1984.tb07531.x
39. De Bock K, Derave W, Ramaekers M, Richter EA, Hespel P. Fiber type-specific muscle glycogen sparing due to carbohydrate intake before and during exercise. Journal of Applied Physiology 2007;102:183–188. https://doi.org/10.1152/japplphysiol.00799.2006
40. Nederveen JP, Ibrahim G, Fortino SA, Snijders T, Kumbhare D, Parise G. Variability in skeletal muscle fibre characteristics during repeated muscle biopsy sampling in human vastus lateralis.

Applied Physiology, Nutrition, and Metabolism 2020;45:368–375. https://doi.org/10.1139/apnm-2019-0263

41. Rosenblueth A, Wiener N. The Role of Models in Science. Philosophy of Science 1945;12:316–321. https://doi.org/10.1086/286874

42. Bazzucchi I, Felici F, Macaluso A, De Vito G. Differences between young and older women in maximal force, force fluctuations, and surface emg during isometric knee extension and elbow flexion. Muscle & Nerve 2004;30:626–635. https://doi.org/10.1002/mus.20151